

Non-Squared Decouple PID Control of Ultra-Compact Binary Power Generation Plant

KUN-YOUNG HAN¹ and HEE-HYOL LEE²

Graduate School of Information, Production and System, Waseda University
2-7 Hibikino, Wakamatsu-ku, Kitakyushu-city, Fukuoka 808-0135, JAPAN

¹kyhan@akane.waseda.jp, ²hlee@waseda.jp

Abstract: This paper deals with making a model and designing a control system of an ultra-compact binary power generation plant using low temperature difference thermal energy. First, a linearized transfer function model of the ultra-compact binary power generation plant is deduced. The model is presented with a linearized transfer function matrix, which represents dynamic characteristics at a neighbor operating point of the investigated plant. Next, a non-squared decouple PID control system is designed. Furthermore, control performance of the control system is investigated.

Keywords—Binary power generation, Linearized transfer function model, Non-Squared (NS) decouple, MIMO system

1 Introduction

Recently, more and more attention has been paid to effective use of renewable energy because of fossil fuels exhaustion problem and environmental issue. The renewable energy source includes temperature difference of thermal energy between deep-sea water and surface seawater, exhaust heat from factories, heat from hot spring, etc. In the power generation using such thermal energy, temperature difference between heat source and cool source is very low compared to the temperature difference in the thermal power generation using fossil fuel or nuclear energy. In the point of view, binary technology is an appropriate method to produce electric power even though the temperature difference between heat source and cool source is very low. Industrial waste heat recovery, binary geothermal power plants, and ocean thermal conversion systems are attempting as examples [1-2].

Up until now, for the power generation using such thermal energy, there has been, on one end, a large-scale geothermal plant class of 1 MW class [3], and on the other end, a small-scale plant of 50 KW class has been developed. However, an ultra-compact scale binary power generation plant of 10KW class, which may be facilitated in small factories or hot-spring guest houses (Onsen Ryokan), is not put to practice. Reasons are as follows: First, a heat-cycle-unit of reasonable cost that can maintain stable power generation is not developed. A heat-cycle-unit includes heat exchanger, turbine, pump, etc. Secondly, there is a problem of selecting suitable working fluid. Thirdly, appropriate control system is not yet developed [4-5].

On the other hands, from the control-engineering point of view, such plant is a complex process

characterized by nonlinearity, uncertainty, and multivariable coupling [7]. Up until the present, PI control strategy of such systems was investigated [6]. However, it is difficult to adaptively tuned proper PI parameters in such system processes owing to multivariable coupling. A multivariable control strategy for a waste heat recovery system was proposed by incorporating a linear quadratic regular (LQR) with the PI controller [7]. In addition, non-linear model has been developed and control method using BP algorithm with non-linear model has been proposed [8-9], but a linear transfer function model that represents the dynamic characteristics of whole power generation system is not yet investigated. Therefore, it is still necessary to develop a properly simplified model to design simple and easily implemented controller.

The aim of this paper is to develop a non-squared (NS) decoupling PID control system for an ultra-compact binary power generation plant and control method to improve the control performance. First, linearized transfer function models that represent dynamic characteristics at an operating point of the ultra-compact binary power plant are deduced to design decoupling PID control system. In addition, NS decoupler to reduce remarkable interaction between controlled variables and manipulated variables are designed. Furthermore, control performance of control system that has a larger number of manipulated variables than the number of controlled variables is investigated to confirm what effect it might have on control performance.

2 An Ultra-Compact Binary Power Generation Plant

2.1 Structure of Power Generation Plant

An ultra-compact binary power generation plant consists of an evaporator, a condenser, a regenerator, a separator, a turbine, pumps of hot water, cold water, and working fluid, and then a working fluid tank as shown in Fig.1. The main manipulated variables of

the ultra-compact binary power generation pilot plant are revolutions of hot water pump and cold-water pump as well as the solenoid valve aperture, while the main controlled variables are a pressure of inlet and outlet of turbine.

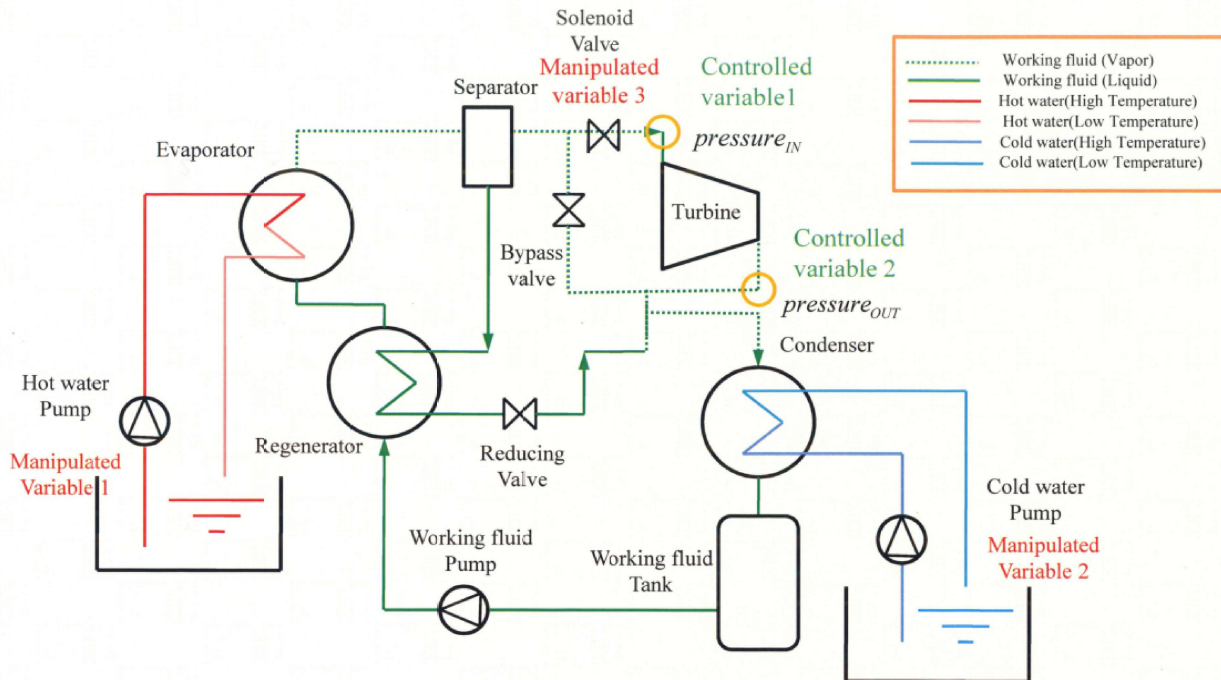


Fig.1. A structure of ultra-compact binary power generation pilot plant

This pilot plant can generate electric power when the pressure difference between the inlet and the outlet of turbine is 400[KPa].

3 Modeling of Ultra-Compact Binary Power Generation Plant

In order to design the control system that controls the pressure of inlet and outlet of the turbine, a mathematical model, which represents dynamic characteristics of the ultra-compact binary power generation plant, is needed. The following sections discuss modeling of the ultra-compact binary power generation plant.

3.1 Measurements of Step Response

Measurements of step response to deduce linearized transfer function matrix models were carried out under the following conditions. First, a step response of the pressure of inlet and outlet of turbine are measured by using flow rate of hot water (60°C) as step input [60 ℓ/min (10Hz) → 283 ℓ/min (60Hz)]. At that time, the flow rate of cold water and working fluid are fixed and a solenoid valve of the inlet of turbine was opened 100 [%]. Next, the flow rate of the cold water (8~9°C) is used as step input [120

ℓ/min (20Hz) → 265 ℓ/min (60Hz)] to measure a step response of the pressure of inlet and outlet of turbine. In addition, the solenoid valve aperture is also used as step input to measure a step response of the pressure of inlet and outlet of turbine. The other variables are fixed. In the measurement, step inputs were put after 2 minutes and the output responses were measured until they reach steady state condition during 4 minutes, and then 240 data were obtained.

3.2 Three Inputs-Two Outputs Transfer Function Model

In this section, the linearized transfer function models of 3 Inputs - 2 Outputs are deduced and the block diagram is shown in Fig.2.

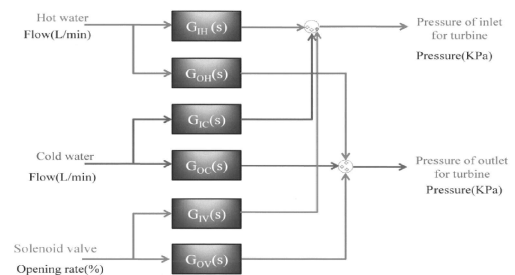


Fig.2. Block diagram of 3 Inputs - 2 Outputs transfer function model

The step responses of the pressure of inlet and outlet of turbine arising from the step inputs of flow rate of hot water, flow rate of cold water, and solenoid valve aperture are shown in Fig.3, Fig.4, and Fig.5, respectively. However, the flow rate of cold-water step input has a negative value because it acts to reduce the pressure of outlet of turbine.

The transfer function models are deduced based on the step response method. First, biases are removed from measured step responses. Secondly, the approximate method using a 1st order time delay and a dead time transfer function using $G_1(s)$ of Eq. (1) is used, and then a 2nd order transfer function $G_2(s)$ is used to express oscillating component. In addition, when the flow rate of hot water is used as the step input, the transfer function models are represented as an integral element as shown as $G_3(s)$ because the responses that rise at constant speed were observed. The deduced transfer function models of the hot water side are connected in parallel.

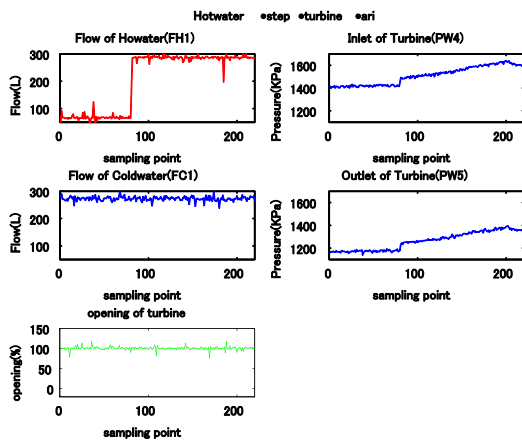


Fig.3. Measured response by hot water step input

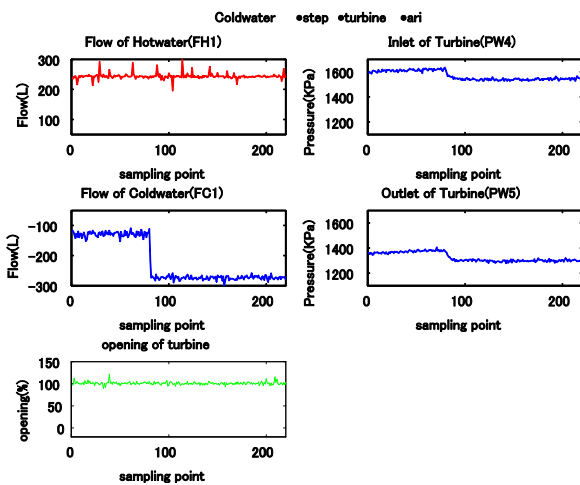


Fig.4. Measured response by cold-water step input

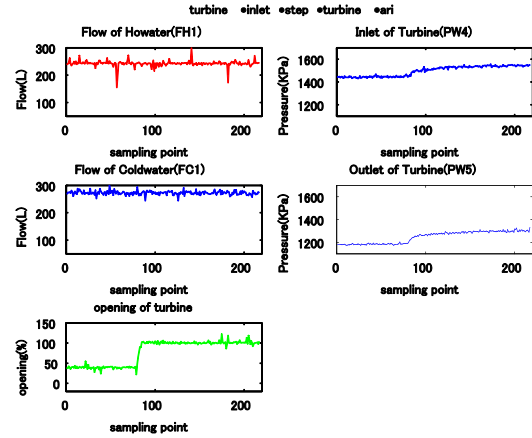


Fig.5. Measured response by solenoid valve step input

$$G_1(s) = \frac{K}{Ts + 1} e^{-Ls}, \quad G_2(s) = \frac{w_n^2}{s^2 + 2\zeta w_n s + w_n^2}, \quad G_3(s) = \frac{1}{Ts} \quad (1)$$

In Eq. (1), T, K, L, w_n , and ζ are time constant, gain, dead time, angular frequency, and damping ratio, respectively. The results that are obtained from the step responses of the pressure of inlet and outlet of turbine by the step input of the flow rate of the hot water are represented in Eq. (2). The transfer function models between the step input of the flow rate of hot water and the pressure of inlet and outlet of turbine are described by parallel connection as shown in Eq. (3). As shown in Eq. (4), the other linearized transfer function models can be deduced in the same manner.

$$G_I(s) = \frac{0.28}{0.01s + 1} e^{-0.01s}, \quad G_2(s) = \frac{12}{s^2 + 1.25s + 12}, \quad G_3(s) = \frac{0.0056}{s} \quad (2)$$

$$G_{IH} = \frac{0.000056s^3 + 0.005663s^2 + 3.367s + 0.0672}{0.01s^4 + 1.007s^3 + 1.245s^2 + 12s} e^{-0.01s} \quad (3)$$

$$G_{OH} = \frac{0.000057s^3 + 0.00574s^2 + 3.14s + 0.0672}{0.01s^4 + 1.007s^3 + 0.81s^2 + 11s} e^{-0.01s}$$

$$G_{IC} = \frac{10}{2.5s^3 + 1.25s^2 + 50s + 20} e^{-0.001s}$$

$$G_{OC} = \frac{3}{2.5s^3 + 2.9525s^2 + 15.77s + 6} e^{-0.001s}$$

$$G_{IV} = \frac{22.5}{11s^3 + 1.22s^2 + 165s + 15} e^{-0.01s}$$

$$G_{OV} = \frac{86.4}{12.5s^4 + 4.5s^3 + 600.3s^2 + 48} e^{0.01s} \quad (4)$$

Comparison of the measured step responses and the step responses of the linearized transfer function models are shown in Fig.6, Fig.7, and Fig.8, respectively.

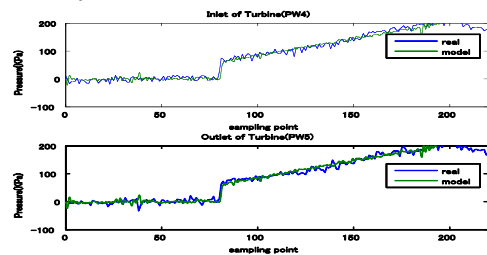


Fig.6. Responses of measurement and model by hot water step input

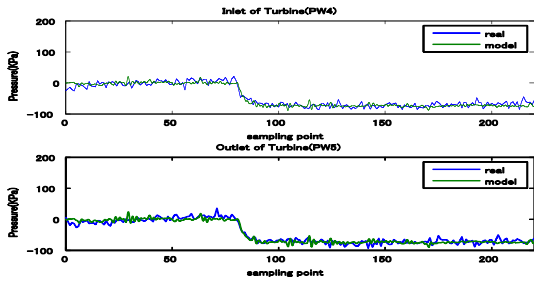


Fig.7. Responses of measurement and model by cold water step input

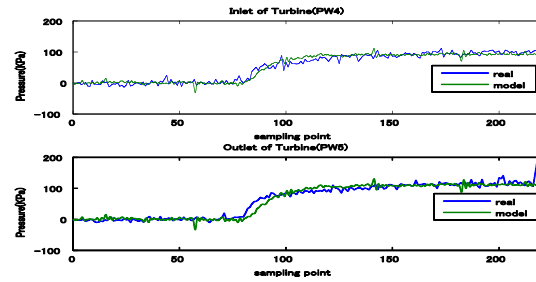


Fig.8. Responses of measurement and model by solenoid valve step input

$$Gp(s) = \begin{bmatrix} \frac{0.000056 s^3 + 0.005663 s^2 + 3.367s + 0.0672}{0.01s^4 + 1.007s^3 + 1.245s^2 + 12s} e^{-0.01s} & \frac{10}{2.5s^3 + 1.25s^2 + 50s + 20} e^{-0.001s} & \frac{22.5}{11s^3 + 1.22s^2 + 165s + 15} e^{-0.01s} \\ \frac{0.000057 s^3 + 0.00574 s^2 + 3.14s + 0.0672}{0.01s^4 + 1.007s^3 + 0.81s^2 + 11s} e^{-0.01s} & \frac{3}{2.5s^3 + 2.9525s^2 + 15.77s + 6} e^{-0.001s} & \frac{86.4}{12.5s^4 + 4.5s^3 + 600.3s^2 + 48s} e^{-0.01s} \end{bmatrix} \quad (5)$$

4 Design of Non-Squared Decouple PID Control System

4.1 PID Control and Decoupling

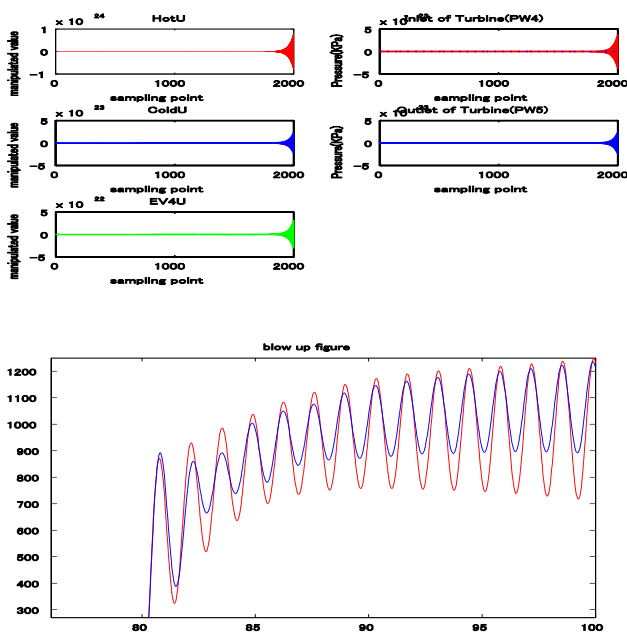


Fig.9. PID control result of 3 Inputs-2 Outputs system

Fig.9 shows the result of PID control for the model of Eq. (5). In this PID control, the other manipulated variables are regarded as disturbance and PID parameters are designed for each loop. In order to obtain good control performance, NS decouplers based on the generalized pseudo-diagonalization method [10] are designed. In Fig.9, the period of oscillation is 1.46 [sec]. A non-interacting pre-compensator Gc_1 is designed by using the hunting

frequency $\omega_{01}=4.3$. The NS decoupler obtained is represented in Eq. (6). In addition, the Inverse Nyquist Array(INA) and Gershgorin bands when pre-compensators and the transfer function models are connected in series are shown in Fig.10.

$$Gc1 = \begin{bmatrix} -0.0127 & -0.7259 \\ -0.2071 & -0.0689 \\ 0.9782 & -0.6843 \end{bmatrix} \quad (6)$$

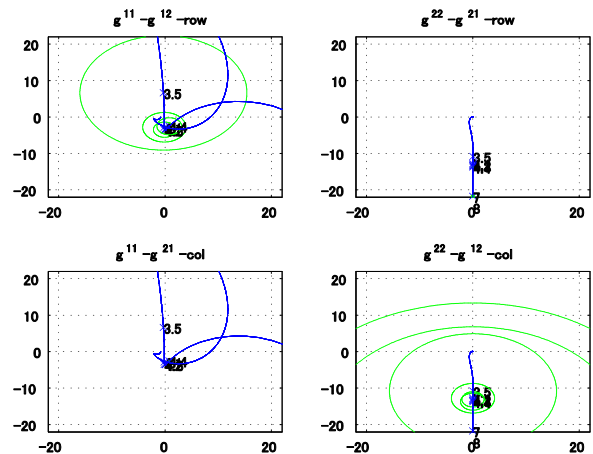


Fig.10. Inverse Nyquist Array and Gershgorin band by Gc_1

4.2 Multi-Stage Connection of Non-Squared Decoupler

In this paper, the multi-stage connection of non-squared decouplers is considered because the Gershgorin bands still include the origin as shown in Fig.10. For the connecting form of NS decoupler, there are series parallel or their combination. In this paper, the parallel connection, which can reduce the oscillating components that cause the interaction on

each other is, used relatively simply [11]. Among the interaction that could not be reduced by one NS decoupler, a particular frequency with remarkable interaction is chosen. For this frequency, new pre-compensator G_{c2} is designed, and then it is connected to G_{c1} in parallel. The block diagram including G_{c1} and G_{c2} is shown in Fig.11. The INA and Gershgorin bands of this system are shown in Fig.12.

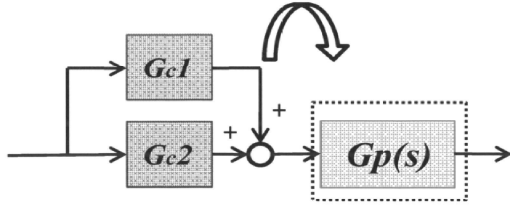


Fig.11. Block diagram of $G_{c1}+G_{c2}$ parallel connection

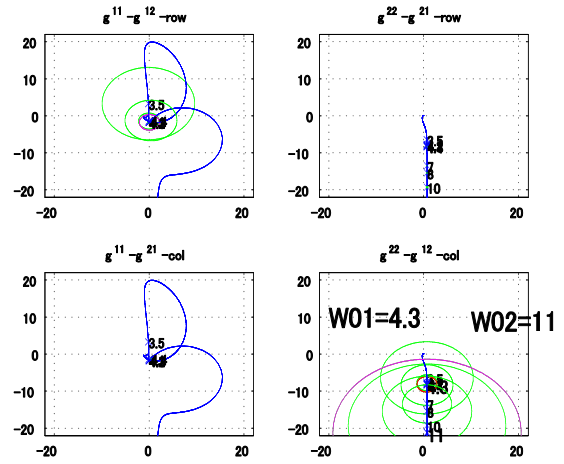


Fig.12. Inverse Nyquist Array and Gershgorin band by $G_{c1}+G_{c2}$

Above process makes Gershgorin bands for $w_{01}=4.3$ and $w_{02}=11$ to not include the origin, and makes the radius of Gershgorin bands of other angular frequencies become smaller. In order to achieve better decoupling effect for $w_{03}=20.0$, $w_{04}=40.0$, $w_{05}=4.1$, $w_{06}=4.4$, and $w_{07}=7.0$, G_{c3} , G_{c4} , G_{c5} , G_{c6} , and G_{c7} are designed and connected in 7-stage parallel connection as shown in Fig.13.

In addition, the INA and Gershgorin bands are shown in Fig.14. The values obtained by connecting 7 non-interacting pre-compensators in parallel are shown in Eq. (7).

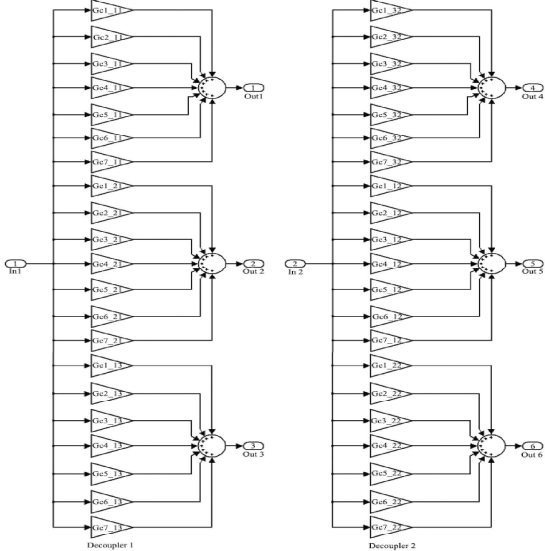


Fig.15. Block diagram of 3 Inputs - 2 Outputs decouple PID control system

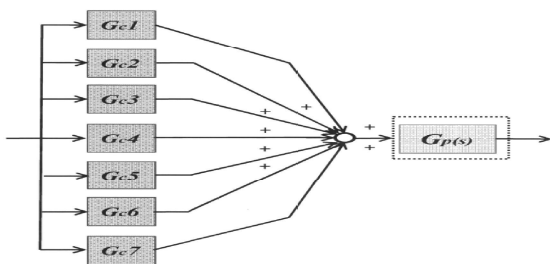
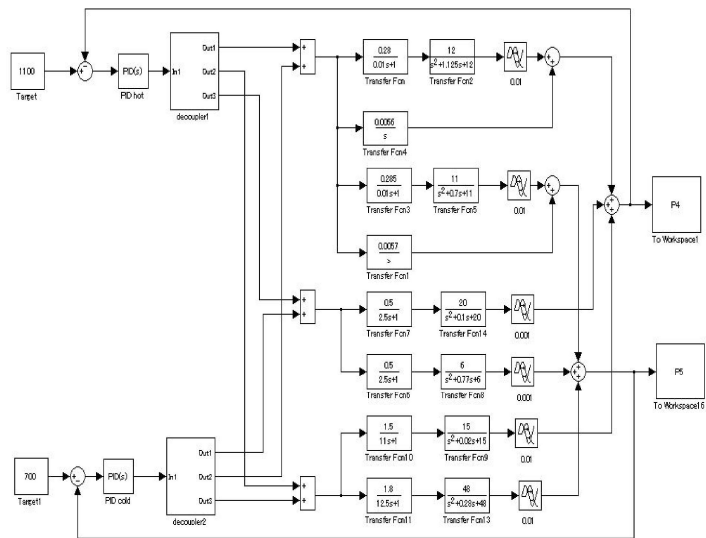


Fig.13. Block diagram of parallel connecting $G_{c1}+G_{c2}+G_{c3}+G_{c4}+G_{c5}+G_{c6}+G_{c7}$

$$G_c = G_{c1} + G_{c2} + G_{c3} + G_{c4} + G_{c5} + G_{c6} + G_{c7}$$

$$= \begin{bmatrix} -0.1086 & 1.6104 \\ -1.4708 & 2.1950 \\ 6.8428 & 3.5541 \end{bmatrix}$$

(7)

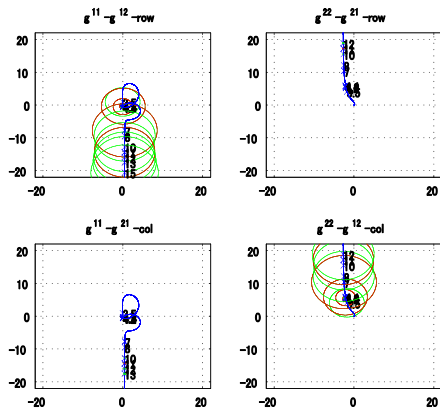


Fig.14. Inverse Nyquist Array and Gershgorin bands by $G_{c1}+G_{c2}+G_{c3}+G_{c4}+G_{c5}+G_{c6}+G_{c7}$

As shown in Fig.14, the diagonal column dominance of $G(s)=Gp(s)(G_{c1}+G_{c2}+G_{c3}+G_{c4}+G_{c5}+G_{c6}+G_{c7})$ is achieved by 7-stage NS decouplers parallel connection because the Gershgorin bands do not include the origin anymore.

4.3 Three Inputs-Two Outputs Decouple PID Control System

A NS decouple PID control system(Fig.15) in which the manipulate variables are flow rate of hot water, cold water, and solenoid valve aperture, and the controlled variables are the pressure of inlet and outlet of turbine. In this section, the controller is designed to make that the pressure of inlet of turbine is 1100 [KPa] and outlet of turbine is 700[KPa]. For the controlled system $G(s)$, PID parameters are designed by using the ultimate sensitivity method. PID parameters are shown in Table1.

Table1. PID Parameters

	3 Inputs – 2 Outputs	3 Inputs – 2 Outputs	2 Inputs – 2 Outputs	2 Inputs – 2 Outputs
	Hot water pump	Cold water pump	Hot water pump	Cold water pump
Kp	0.04	0.66	0.05	1.84
Ti	0.70	0.45	0.20	14.61
Td	0.18	0.11	0.05	0.80

4.4 Two Inputs-Two Outputs Decouple PID Control System

In order to examine the effect of number of manipulated variables on control performance, 2 Inputs - 2 Outputs Decouple PID control system, in which the manipulated variables are flow rate of hot water and flow rate of cold water which has less manipulated variables than 3 Inputs - 2 Outputs system, is considered. Similarly, for the case of 3 Inputs - 2 Outputs system, 2 Inputs - 2 Outputs

decouple PID control system using 7-stage parallel connection of NS decouplers are designed. PID parameters are again designed by using the ultimate sensitivity method. PID parameters are shown in Table1.

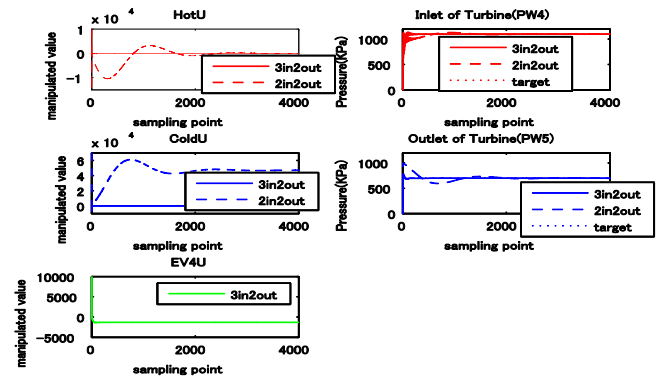


Fig.16. Comparison of control performance

4.5 Comparison of Decouple PID Controls

The results of NS decouple PID control for 3 Inputs - 2 Outputs system and 2 Inputs - 2 Outputs system are compared as shown in Fig.16. From Fig.16, it can be observed that the settling times are about 700 [sec] and about 2200 [sec], respectively. From this result, we can know that 3 Inputs - 2 Outputs system has better control performance because the settling time is reduced to about 30%.

4.6 Examination of Control Performance

In this section, the control performance of 3 Inputs - 2 Outputs system and 2 Inputs - 2 Outputs system are compared by using the gain margin and phase margin. The Nyquist diagram and the Bode diagram of open loop for hot water loop and cold-water loop of 3 Inputs - 2 Outputs system are shown in Fig.17 and Fig.18, respectively.

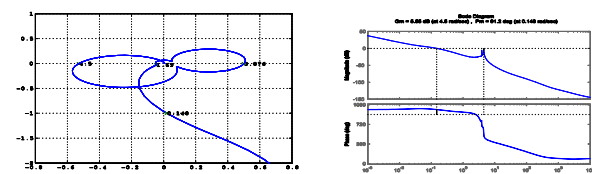


Fig.17. Nyquist and Bode diagram of hot water loop of 3 Inputs - 2 Outputs system

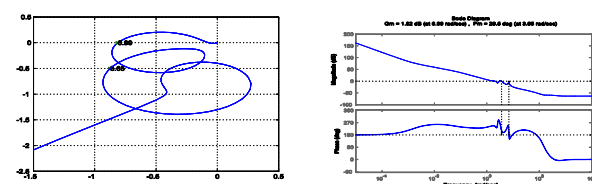


Fig.18. Nyquist and Bode diagram of cold water loop of 3 Inputs-2 Outputs system

Table2. Comparison of control performance

Control Performance	Desired value	Classification	3I-2O	2I-2O
Gain Margin	3~10 [dB]	Hot Water	5.55 [dB]	0.262 [dB]
		Cold Water	1.82 [dB]	48.2 [dB]
Phase Margin	20~70 [dB]	Hot water	91.2 [deg]	4.17 [deg]
		Cold water	29.5 [deg]	19.6 [deg]
Settling Time			700 [sec]	2,200 [sec]

Table 2 shows the result of comparison for control performance. The gain margin of hot water loop at -180 [°] with $\omega=4.5$ [rad/sec] is 5.55 [dB], and the gain margin of cold-water loop at $\omega=6.99$ [rad/sec] is 1.82 [dB]. From the result, it can be confirmed that the gain margins of the 3 Inputs - 2 Outputs decouple PID control system are nearer to desired values and that the control performance is better.

5 Conclusion

The linearized transfer function models that represent dynamic characteristics at the operating point of the ultra-compact binary power generation using low temperature difference thermal energy were deduced. The step responses from the models were compared with the measured step responses from experiment to confirm the validity of models. The NS decouplers were designed to remove the remarkable interaction between controlled variables and manipulated variables. The NS decouple PID control system was designed to control the pressure difference between the inlet and outlet of turbine to keep to 400[KPa] by the high pressure, steam of working fluid, and then its control performance was demonstrated. Through the simulation, the effectiveness of the proposed 3 Inputs - 2 Outputs NS decouple PID control system was examined and confirmed by comparing the results with that of the 2 Inputs - 2 Outputs decouple PID control system.

References:

- [1] Power Engineering, "New Ways to produce Geothermal Power at Lower Temperature", http://www1.eere.energy.gov/geothermal/news_detail.html?news_id=19207.
- [2] BF.Tchanche, Gr.Lambrinos, A. Frangoudakis, G.papadakis, "Low-grade heat conversion into power using organic Rankine Cycle-A review of various applications", Science Direct, Appl Energy, vol.15, no.88, pp2963-3979, 2011.
- [3] DiPippo R. Geothermal power plants, "principles, application case studies and environmental impact", Elsevier, 2008.
- [4] NEDO Renewable Energy Report, "art1, the role of renewable energy", <http://www.nedo.go.jp/content/100544816.pdf>.
- [5] SHIZUOKA PREPECTURE, "Report on the Possibility of Introducing of business of power generation using hot spring thermal energy", <http://www.pref.shizuoka.jp/kigyuu/documents/h22gaiyo.pdf>.
- [6] Quoilin S, Aumann.R, Grill A, Schuster A, Le, mort V, Spliethoff.H, "Dynamic modeling and optimal control strategy of waste heat recovery organic Rankine cycles", Science Direct, Apply energy, vol.88, no.6, pp.2183-2190, 2011.
- [7] Zang. J, Zhang.W, Hou.G, Fang.F, "Dynamic modeling and multivariable control of organic Rankine cycle in waste heat utilizing processes", Science Direct, Computer math with App, vol.64, no.5, pp.908-921, 2012.
- [8] L. Owens, "OTEC plant response and control analysis", AS ME J Solar Energy Eng., vol.104, no.3, pp.208-215, 1982.
- [9] Stomi S, Han K-Y, S J-S, Lee H-H, "A learning control of unused energy power generation", Journal of AROB, vol.15, no.4, pp.450-454, 2010.
- [10] H-H Lee, W-K Choi, J-Y Song, S-G Lee, Akizuki K, "Noninteracting PID Control of a Fluid Temperature and Liquid Level Interacting System", Trans. IEE of Japan, vol.119-C, no.8/9, pp.1035-1041, 1999.
- [11] H-H Lee, Nagamachi M, W-K Choi, J-Y Song, Miyazaki M, Akizuki K, "Noninteracting Multi-Stage Noninteracting PID Control by Precompensators with Series-Parallel Connection", Trans. IEE of Japan, vol.123, no.1, pp.43-49, 2003.